

## Video imaging of the sperm acrosome reaction during in vitro fertilization

Noritaka Hirohashi,<sup>1\*</sup> George L. Gerton<sup>2</sup> and Mariano G. Buffone<sup>3</sup>

<sup>1</sup>Department of Biological Sciences; Graduate School of Humanities and Sciences; Ochanomizu University; Bunkyo, Tokyo Japan; <sup>2</sup>Department of Obstetrics and Gynecology; Center for Research on Reproduction and Women's Health; University of Pennsylvania School of Medicine; Philadelphia, PA USA; <sup>3</sup>Instituto de Biología y Medicina Experimental; National Research Council of Argentina (CONICET) Vuelta de Obligado; Aires, Argentina

**M**ammalian spermatozoa become competent for fusion with oocytes while traveling through the female reproductive tract and the oocyte's extracellular investments. Recent studies highlighted the molecular mechanism of the sperm's interactions with the zona pellucida (ZP), the extracellular coat surrounding the oocyte. Fertilizing spermatozoa initiate the sperm acrosome reaction (AR), essential for zona penetration and fusion with the oocyte plasma membrane, before they reach the ZP. However, the exact condition of spermatozoa that leads to successful penetration of the ZP remains unknown. We performed microscopic observations of in vitro fertilization with genetically (EGFP) and chemically (antibody and lectin) labeled spermatozoa to monitor the progression of the AR. Spermatozoa exhibiting EGFP/PNA<sup>+</sup> prior to binding to the ZP initiated zona penetration. This result suggests that spermatozoa that have undergone the AR are still capable of binding and penetrating the ZP.

Specific adhesion of spermatozoa to the oocyte's extracellular coat, the zona pellucida (ZP) is an essential process for mammalian fertilization. Therefore, the molecular nature of sperm-ZP interactions (components of the ZP as well as in the sperm plasma membrane fractions) has been extensively studied in various species of eutherian mammals. In mice, the ZP sialoglycoprotein ZP3 is the sperm receptor.<sup>1</sup> Contrary to this relatively simple situation, there are more than two dozen

candidates that have been claimed to be ZP (ZP3) receptors in various mammalian species.<sup>2</sup>

One paradigm considers the ZP receptor(s) to be localized on the plasma membrane of acrosome-intact spermatozoa, which derived from observations that acrosome-intact spermatozoa adhere to the ZP during in vitro fertilization (IVF). Subsequently, the sperm acrosome reaction (AR) is believed to occur on the ZP surface. Underpinning with this view, a large number of reports demonstrate that ZP3 is the inducer of the sperm AR.<sup>3</sup> Thus, the theoretical model of sperm-egg interactions has been formed based on discontinuous observations of some key events during IVF. However, using transgenic mice and retrospective video-imaging microscopy, we recently reported that fertilizing spermatozoa initiated the acrosome reaction (as defined by a loss of acrosomal EGFP) before their contact with the ZP.<sup>4</sup> These observations raise the question of whether fertilizing spermatozoa, prior to contact with the ZP, have begun or completed acrosomal exocytosis. In this report, we performed real-time assessment of the acrosome status of living spermatozoa approaching and thereafter contacting the ZP of the cumulus-oocyte complex (COC).

Recent studies highlighted that the AR is not a binary event (acrosome being either completely intact or totally reacted), but rather constitutes a continuum of different states.<sup>5</sup> We investigated cell surface staining for acrosomal makers, i.e., sp56/ZP3R and peanut agglutinin lectin

**Key words:** acrosome reaction, sperm, live-cell imaging

Submitted: 03/25/11

Accepted: 03/25/11

DOI: 10.4161/cib.4.4.15636

\*Correspondence to: Noritaka Hirohashi;  
Email: hirohashi.noritaka@ocha.ac.jp

Addendum to: Jin M, Fujiwara E, Kakiuchi Y, Okabe M, Satoh Y, Baba SA, et al. Most fertilizing mouse spermatozoa begin their acrosome reaction before contact with the zona pellucida during in vitro fertilization. *Proc Natl Acad Sci USA* 2011; 108:4892-6; PMID: 21383182; DOI: 10.1073/pnas.1018202

**Figure 1 (See opposite page).** Histochemical dissection of the acrosomal exocytosis. (A) The diagram shows the temporal correlation between progression of the acrosomal exocytosis and the surface exposure of intra-acrosomal markers suggested by this study. An intra-acrosomal protein, sp56/ZP3R is exposed on the sperm surface before initiation of the acrosomal exocytosis as judged by the presence of soluble acrosomal EGFP fluorescence. Whereas, peanut agglutinin lectin (PNA)-reactive carbohydrate residues, that locate inside the acrosome, is exposed to the apical ridge subdomain (white arrowhead) after disappearance of EGFP fluorescence, followed by extended staining to the equatorial segment (yellow arrowhead) of sperm head, which is regarded as completion of the acrosomal exocytosis.<sup>13</sup> Although such equatorial staining was clearly seen under a fluorescence microscope, neither flow cytometry analysis nor PNA-MIVF assay could distinguish between early and late stages of PNA distributions (see below). Mitochondria were labeled with Ds-Red2. (B) Staining of transgenic sperm with Qdot® 800-labeled PNA revealed that PNA<sup>+</sup> and EGFP<sup>+</sup> sperm were mutually reciprocal. B/G, a dual G/B excitation filter; IR, a near-infrared filter. Scale bars; 10 μm. (C) In contrast, vital staining with anti-sp56 antibody revealed at least four major types of sperm populations, i.e., EGFP<sup>+</sup>/sp56<sup>-</sup>, EGFP<sup>+</sup>/sp56<sup>+</sup>, EGFP<sup>-</sup>/sp56<sup>+</sup> and EGFP<sup>-</sup>/sp56<sup>-</sup>. (D) Flow cytometry of transgenic sperm showed only two major groups (EGFP<sup>+</sup>/PNA<sup>-</sup> and EGFP<sup>-</sup>/PNA<sup>+</sup>) in capacitating population. Capacitation time was indicated in each part. (E) In contrast, a broad distribution of sp56-positive sperm was observed in both in EGFP<sup>+</sup> and EGFP<sup>-</sup> populations. Color bar, sperm density. (F) Histograms of the fluorescence intensity (FL3) showed two distinct bell-shaped distributions in PNA<sup>+</sup> sperm population, whereas a scattered distribution of sp56<sup>+</sup> sperm was observed. These results agree with microscopic observations by which heterogeneities of the staining intensity and pattern in sp56<sup>+</sup> sperm were identified (data not shown).

(PNA)-reactive carbohydrates in sperm populations under capacitating conditions where spermatozoa trigger the spontaneous AR. PNA-positive (PNA<sup>+</sup>) spermatozoa are regarded as having undergone the AR as defined by externalization of the acrosomal constituents,<sup>4,6</sup> whereas sp56/ZP3R is exposed to the cell surface before soluble EGFP is diffused away from the acrosome<sup>7</sup> and released in progressive stages (Fig. 1A).<sup>8</sup> Analyses with fluorescence microscopy (Fig. 1B and 1C) and flow cytometry (Fig. 1D and 1E) revealed progressive changes in acrosomal antigens on the sperm surface, confirming the results previously presented. Notably, at any time point following capacitation, spermatozoa that exhibit both EGFP<sup>+</sup> and PNA<sup>-</sup>, representing an intermediate state of the AR, were rarely observed (Fig. 1B), suggesting a rapid transition from EGFP<sup>+</sup>/PNA<sup>-</sup> to EGFP<sup>-</sup>/PNA<sup>+</sup> during the spontaneous AR.

We next developed assays for visualizing the acrosome status of living spermatozoa during passage through the cumulus cell layer (CCL). First, anti-sp56/ZP3R antibody or PNA was coupled to fluorescent polystyrene microspheres<sup>9</sup> by which the acrosomal status of sperm population entering in the CCL could be analyzed statistically by counting the number of beads carried by spermatozoa (Fig. 2A). In this assay, we found that large populations of sp56/ZP3R-exposed and/or PNA antigen-exposed spermatozoa could enter the CCL, suggesting that acrosome-reacted or acrosome-reacting spermatozoa were capable of entering and passing through the cumulus matrix (Fig. 2B and C). Second, microscopic IVF (MIVF) was performed in the presence of Alexa

594-labeled PNA, by which a real-time imaging of the acrosomal status and even its transition are enabled at the zona periphery (Fig. 3A). Transition from acrosome-intact (EGFP<sup>+</sup>) to acrosome-reacted (PNA<sup>+</sup>) was rarely seen in the vicinity of the ZP (3 cases in 17 experiments) and the time required for such transition was approximately 2 min (Fig. 3C). In this assay, among EGFP<sup>+</sup> sperm that had bound to the ZP, PNA<sup>+</sup> spermatozoa were most abundant (91.2%), whereas there were small numbers of double-negative (i.e., transitional state of EGFP<sup>+</sup>/PNA<sup>-</sup>) spermatozoa (Fig. 3B). Among PNA<sup>+</sup>, ZP-bound spermatozoa, only 4% initiated penetration through the ZP (5/125, Fig. 3D and E).

The long-standing conceptual view that the soluble acrosomal lysins create a path in the ZP, which facilitates sperm penetration through the egg extracellular matrix, imposes that the AR must be triggered in the close vicinity of the target for lytic action (i.e., the ZP). However, recent investigations call into a question whether soluble components housed in the acrosome play a role in egg-coat lysis. More importantly, sperm take a considerable period of time to complete the sequential processes of membrane fusions, time-dependent exposure and release of intra-acrosomal proteins and post-translational modifications of cell surface antigens.<sup>8,10</sup> The relationship of the progression of the AR to the penetration of the ZP and fusion with the oocyte remains unknown. Several laboratories reached the same conclusion that sperm binding to the ZP is not sufficient for the AR induction.<sup>11</sup> We recently found that most fertilizing spermatozoa initiate the AR before they reach

the ZP.<sup>4</sup> Therefore, it is important to determine acrosomal status at the moment of sperm contact with the ZP. To address these questions, we performed live-cell imaging with transgenic sperm and chemical probes to detect cell surface antigens. Acrosome staining with PNA would represent sperm that have undergone the AR and proceeded to the advanced stages following point fusions between the outer acrosomal membrane and the plasma membrane.<sup>12</sup> Early stages of the AR can be defined by absence of both GFP and PNA fluorescence, which was observed in a minor population of sperm during MIVF (Fig. 3B). The majority of GFP-spermatozoa exhibited PNA fluorescence when they made contact with the ZP. Although the extent of original membrane loss remains to be identified, our studies provide the first blueprint of physiological changes associated with the acrosomal exocytosis in fertilizing spermatozoa. In a perspective view, electron microscopy analysis in conjunction with live-cell imaging would be useful to identify the precise status of the acrosome at the moment of gamete interaction. This would give new insights into the cellular and molecular bases of mammalian fertilization.

#### Acknowledgments

We thank Dr. Vic Vacquier for his critical reading of the manuscript. This study was supported by the Japan Society for the Promotion of Science (N.H.).

#### References

1. Litscher ES, Williams Z, Wassarman PM. Zona pellucida glycoprotein ZP3 and fertilization in mammals. *Mol Reprod Dev* 2009; 76:933-41.
2. Reid AT, Redgrove K, Aitken RJ, Nixon B. Cellular mechanisms regulating sperm-zona pellucida interaction. *Asian J Androl* 2011; 13:88-96.

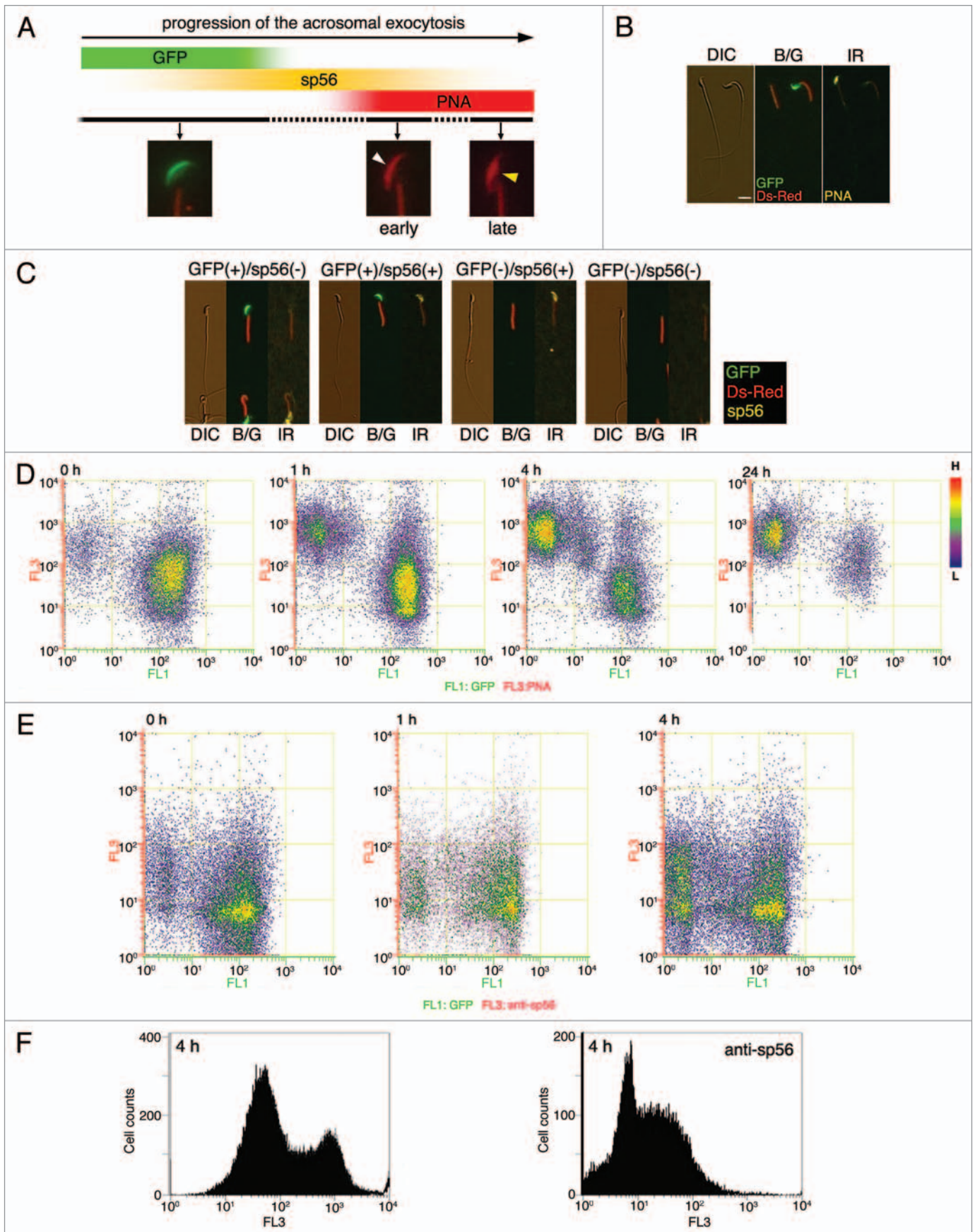


**Figure 1.** For figure legend, see previous page.

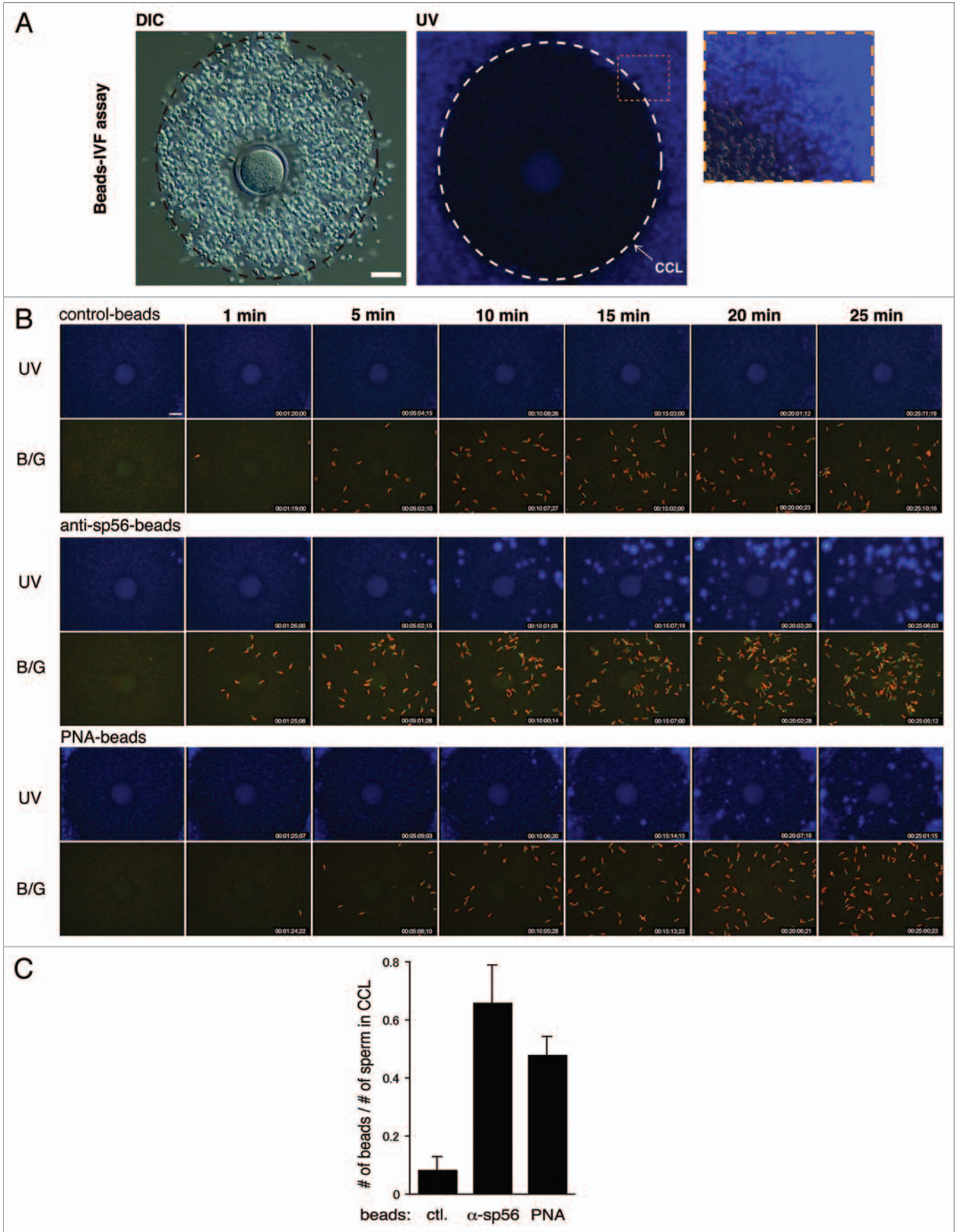


**Figure 2 (See opposite page).** Bead-MIVF assay. (A) Low magnification views (left and center) of the COC in medium containing protein-coupled fluorescent beads. Images were taken by differential interference contrast microscopy (DIC) and fluorescence microscopy with an ultraviolet (UV) filter. An outer edge of the CCL (center, inset) was enlarged (right). No beads were found in the CCL, indicating that 0.5  $\mu\text{m}$  polystyrene microparticles (Polysciences) cannot penetrate the cumulus matrix by free diffusion. (B) Capacitated spermatozoa were thereafter inseminated and their entry into the CCL was monitored to determine if the beads were carried by CCL-entering sperm. Beads used were control IgG beads, anti-sp56 beads and PNA beads. Photographs were taken every 5 min using fluorescence microscopy with a UV filter or a dual band-pass filter (B/G). (C) After 30 min of insemination, the fluorescent beads and sperm within the CCL were counted and the bead/sperm ratio calculated. The data are expressed as the mean ratio of beads/sperm  $\pm$  SEM obtained from 4 independent experiments. Scale bars: 50  $\mu\text{m}$ .

3. Gupta SK, Bhandari B. Acrosome reaction: relevance of zona pellucida glycoproteins. *Asian J Androl* 2011; 13:97-105.
4. Jin M, Fujiwara E, Kakiuchi Y, Okabe M, Satoh Y, Baba SA, et al. Most fertilizing mouse spermatozoa begin their acrosome reaction before contact with the zona pellucida during in vitro fertilization. *Proc Natl Acad Sci USA* 2011; 108:4892-6.
5. Buffone MG, Foster JA, Gerton GL. The role of the acrosomal matrix in fertilization. *Int J Dev Biol* 2008; 52:511-22.
6. Kallajoki M, Virtanen I, Suominen J. The fate of acrosomal staining during the acrosome reaction of human spermatozoa as revealed by a monoclonal antibody and PNA-lectin. *Int J Androl* 1986; 9:181-94.
7. Kim KS, Foster JA, Gerton GL. Differential release of guinea pig sperm acrosomal components during exocytosis. *Biol Reprod* 2001; 64:148-56.
8. Buffone MG, Kim KS, Doak BJ, Rodriguez-Miranda E, Gerton GL. Functional consequences of cleavage, dissociation and exocytotic release of ZP3R, a C4BP-related protein, from the mouse sperm acrosomal matrix. *J Cell Sci* 2009; 122:3153-60.
9. Kim KS, Gerton GL. Differential release of soluble and matrix components: evidence for intermediate states of secretion during spontaneous acrosomal exocytosis in mouse sperm. *Dev Biol* 2003; 264:141-52.
10. Honda A, Siruntawinetti J, Baba T. Role of acrosomal matrix proteases in sperm-zona pellucida interactions. *Hum Reprod Update* 2002; 8:405-12.
11. Gahlay G, Gauthier L, Baibakov B, Epifano O, Dean J. Gamete recognition in mice depends on the cleavage status of an egg's zona pellucida protein. *Science* 2010; 329:216-9.
12. Yanagimachi R. Mammalian fertilization. *The Physiology of Reproduction*. Knobil E, Neil J, Eds. New York: Raven 1994; 189-317.
13. Cheng FP, Fazeli AR, Voorhout W, Bevers MM, Colenbrander B. Use of PNA (peanut agglutinin) to assess the acrosomal status and the zona pellucida induced acrosome reaction in stallion spermatozoa. *J Androl* 1996; 17:674-82.

**Figure 3 (See following page).** PNA-MIVF assay. (A) Low magnification views of the COC in medium containing Alexa 594-labeled PNA under DIC (left) and fluorescence (right) microscopy with a dual band-pass filter (B/G). An outer border of the CCL was marked (dashed circle). In contrast to the bead-IVF assay, PNA could penetrate the cumulus matrix and stained the ZP. In comparison to the high red fluorescence background (due to presence of Alexa-PNA) in the CCL, the zona periphery was relatively dark, providing an opportunity to detect the acrosomal status of sperm arriving at this area. (B) Among EGFP<sup>-</sup> sperm that bound to the ZP, most were PNA<sup>+</sup>, whereas approximately 10% were PNA<sup>-</sup>. (C) A representative case of a sperm that underwent the AR while traveling through the zona periphery. Shown are the full screen image of the COC in this experiment (left) and enlarged (boxed area) time-lapse images of the spermatozoon undergoing the AR (right). A gradual disappearance of the acrosomal green fluorescence (8 min 9 s) followed by accumulation of red fluorescence (9 min 54 s) was observed. Color in the acrosome was shown as a bar below each photograph. (D) Representative photographs of the consecutive processes from sperm passage through the CCL to sperm binding to the ZP by PNA<sup>+</sup> sperm. (E) Out of 125 PNA<sup>+</sup> ZP-bound sperm, 5 sperm initiated ZP-penetration. Arrowheads point to the acrosomal region; scale bar, 50  $\mu\text{m}$ .

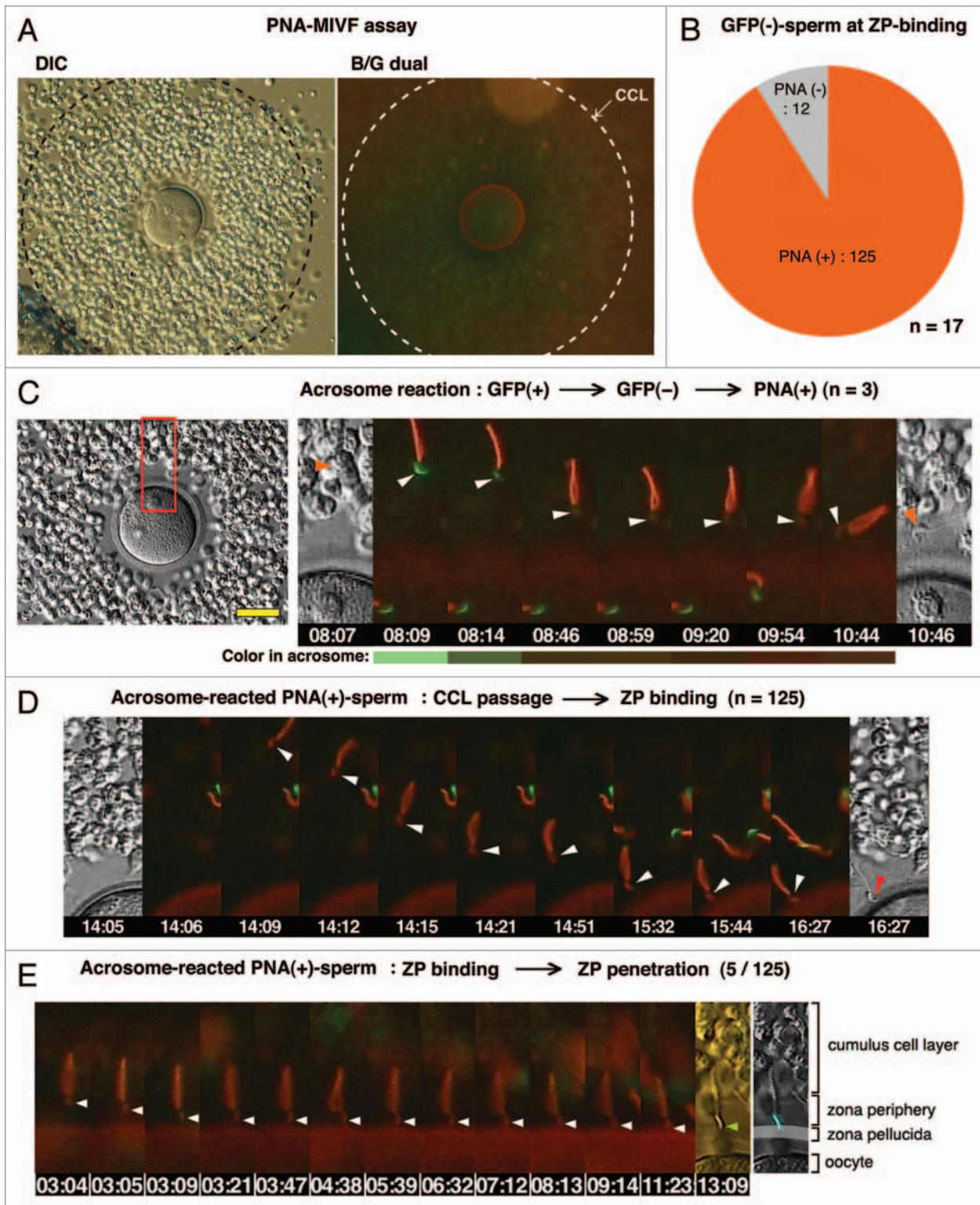


**Figure 3.** For figure legend, see previous page.